Journal of Porous Media 7(4), 1–14 (2004)

Convection and Dispersion in a Naturally Fractured Reservoir

E. Luna[1*], A. Medina[1], C. Pérez-Rosales[1], and C. Treviño[2]

[1]Instituto Mexicano del Petróleo, YNF. 07730 México D.F., México
[2]Facultad de Ciencias, UNAM. 04510 México D.F., México
[*]E-mail: eluna@imp.mx

ABSTRACT

In this work, theoretical and experimental studies are presented on the natural convection flow in a naturally fractured reservoir, produced by a vertical geothermal gradient. The present approach considers finite oil-filled, tilted fractures with small aspect ratios, with a fluid thermal conductivity assumed to be very small compared with the thermal conductivity of the rock matrix. These assumptions are fully justified for actual Mexican naturally fractured reservoirs. Finite tilted porous layers saturated with oil have also been considered. In all the cases studied, convection occurs under any vertical temperature gradient. In addition, the diffusion and dispersion of nitrogen (N_2) is studied, with this substance located initially at the top of the fracture. In these types of flows, the influence of convection over diffusion and dispersion of passive substances is extremely small.

Keywords: Thermal convection; Reservoir engineering; Enhanced oil recovery

AUTHER:
[T1]Is this new line correct?

Received February 24, 2004; Accepted June 20, 2004

NOMENCLATURE

C^*	dimensional mass concentration
C	dimensionless mass concentration
c_v	specific heat of constant fluid volume
D_d	dispersion coefficient
D	diffusion coefficient (or effective diffusion coefficient in a porous medium)
d	fracture width
G	temperature gradient
g	gravity acceleration
H	height of the solid block (matrix)
h	fracture length
K	permeability of the porous medium
k_f	fluid thermal conductivity
k_T	overall thermal conductivity
k_s	rock thermal conductivity
L	solid length
Y	dimensionless mass concentration
p_0	dimensionless, zeroth-order effective pressure in the porous layer
p_1	dimensionless, first-order effective pressure in the porous layer
p^*	dimensional pressure
p	dimensionless pressure
p_c	characteristic pressure
t^*	dimensional time
t	dimensionless time
t_{cD}	characteristic diffusive time
t_{cC}	characteristic convective time
u_c	characteristic velocity (characteristic filtration velocity field in the porous medium)
u_0	dimensionless, zeroth-order filtration velocity
u_1	dimensionless, first-order filtration velocity
(u^*, v^*)	dimensional, two-dimensional velocity field (or filtration velocity field in the porous medium)
(x^*, y^*, z^*)	dimensional, fracture coordinates
(x_1^*, y_1^*, z_1^*)	dimensional, left-hand-side coordinates of the solid
(x_2^*, y_2^*, z_2^*)	dimensional, right-hand-side coordinates of the solid
(x, y, z)	dimensionless, fracture coordinates
(u, v)	dimensionless velocity field (or dimensionless filtration velocity field in the porous medium)
(x_1, y_1, z_1)	dimensionless, left-hand-side coordinates of the solid
(x_2, y_2, z_2)	dimensionless, right-hand-side coordinates of the solid
S_i	separation surface between the slab and the solid matrix (i = 1 LHS fracture's wall and i = 2 RHS fracture's wall)
T_H	temperature at the lower part of the solid
T_C	temperature at the upper part of the solid
T_0	temperature of reference
Pr	Prandtl number
Ra	Rayleigh number
Pe_α	dispersive Peclet number
Pe	diffusive Peclet number
Pe_T	thermal Peclet number in the matrix

Greek letters

α	dispersivity coefficient
β	thermal volume expansion coefficient

θ	dimensionless temperature in the fluid	Γ	aspect ratio of the tilted cavity (fracture, vug, or porous layer)
σ	convective dimensionless time (fluid-filled cavity)	Θ_i	second-order dimensionless temperature in the solid matrix obtained through numerical method
σ_p	convective dimensionless time (saturated porous layer)	φ	first-order stream function
θ_i	dimensionless temperature on the part *i* of the solid	$\Delta = (T_H - T_C)$	temperature difference
Φ	fracture inclination angle	(ξ_i, η_i)	rescaled coordinates of part *i* of the solid
φ	fracture porosity	**Subscripts**	
κ_f	fluid thermal diffusivity	*i*	refers to each part (*i* = 1 left-hand side
κ_T	overall thermal diffusivity		or *i* = 2 right-hand side) of the solid
κ_s	rock thermal diffusivity	*f*	refers to the fluid
μ	dynamic viscosity	*s*	refers to the solid
ν	kinematic viscosity		
ψ	stream function	**Superscripts**	
ρ_0	reference density	*	refers to dimensional quantities
τ	porous medium tortuosity		

1. INTRODUCTION

It is well known that an oil reservoir is subjected (in absence of near hot bodies) to a vertical temperature gradient *G*, the geothermal gradient, which is approximately constant (see, for instance, Phillips, 1991). This thermal gradient produces changes in the fluid density and thus self-organized, cellular, convective currents (Nield and Bejan, 1998; Phillips, 1991) can be developed in the oil-saturated homogeneous porous medium. To our knowledge, the researchers who initially determined the critical value of the Rayleigh number Ra_c (a dimensionless parameter that relates the body to viscous forces) were Horton and Rodgers (1945) and independently Lapwood (1948) (HRL problem). In fact, they have determined that the minimum value of the Rayleigh number to start the convective motion is given by $Ra_c = 4\pi^2$. This result is similar to the convective problems, where gaps are filled with viscous fluids, under the action of vertical temperature gradients (Rayleigh–Benard problem). When the gap has infinite width and finite height, the well-known critical Rayleigh number is $Ra_c = 1708$. On the other hand, if the temperature gradient is horizontal along a finite gap (for example, different temperatures on the two parallel walls of the gap) the convective motion occurs for any value of the Rayleigh number, even if it is very small, i.e., there is no critical Rayleigh number (Bejan, 1995).

The field of thermal convection in fractured reservoirs is very important in petroleum engineering, but has been scarcely studied in the past. The present work will show that the study of convection in a single, finite fracture is sufficient to understand the main aspects of the convection in the overall fractured reservoir. In this sense, it is pertinent to comment that the present work is based partially on the archetypal problem of an infinite tilted fracture treated ten years ago for a fluid-filled fracture and for a tilted, saturated porous layer by Woods and Linz (1992) and Linz and Woods (1992), respectively. In those works, they have considered infinite-length fractures immersed in an infinite solid and, under this approximation, they determined that the convective motion always occurs (as in the case of a gap with horizontal gradient). The cause of this phenomenon is that the isotherms are shifted close the fracture. In the present work, it has been considered the

approximation of an impervious rock (solid) of finite dimensions, which is subjected to an imposed vertical temperature gradient $G = \Delta T/H$, where ΔT is the overall temperature difference between the bottom and the top of the reservoir and H represents its height.

In Section 2, the governing equations for the fluid and the solid are formulated. Assuming that the solid has an embedded, tilted slab of finite length h and width d, and that the material within the slab has very different thermal conductivity in comparison with that of the rock itself, it is shown that a noticeable distortion occurs in the isotherms around the fracture. In short, it gives rise to a system where the convection always exists. In general, the aspect ratio $\Gamma = d/h$ and the ratio of the thermal conductivity of the fluid k_f, to that of the rock k_s are very small compared with unity. For instance, limestone has a thermal conductivity around ten times that of oil and so $\kappa = k_f/k_s << 1$ (Bear, 1972; Davies et al., 1981).

In most cases of interest in connection with fractured oil reservoirs, both Γ and κ are small compared with unity. But, given the large variety of oil-filled slabs present in a reservoir, the ratio of these two parameters may span a wide range of values, both large and small compared with unity. In the case of κ small compared with Γ, the heat conduction across the slab can be neglected and the temperature in the solid around the slab T_s satisfies Laplace's equation with adiabatic boundary conditions at the fracture interface. The formal treatment and justification of this approximation for an oil-filled slab like an oil-filled vug ($\Gamma \sim 1$) will be given in Section 3. This procedure is only useful for the case of a vug and it is not useful for solving the problems of convective flow in slim fractures ($\Gamma << 1$) and in oil-saturated porous layers. The theoretical treatment of the convection will be given in all cases as a combination of analytical, asymptotic, and numerical techniques, and detailed developments will be presented in Section 4, for convection in a vug and in a slim fracture. The study of convection in a tilted porous layer will be given in Section 4. The manner in which dispersion (or transport) of a passive substance occurs due to the simultaneous presence of molecular diffusion and natural convection within the cavities will be discussed in Section 5. This latter study now has an enormous impact due to the novel enhanced oil-recovery procedures used in naturally fractured reservoirs. Finally, the conclusions and some very important remarks in relation to the convection and dispersion in actual reservoirs will be given in Section 6.

2. THEORETICAL MODEL FOR A TILTED SLAB

The archetypal system to be analyzed is a block of finite width L and height H with $L >> H$ and infinite depth in order to have an effective two-dimensional flow in a tilted fracture, under a vertical temperature gradient G. In Fig. 1a, the coordinate systems, the dimensions of the block, and the fracture (tilted slab) are shown, together with the corresponding physical properties of the fluid and the block. The temperature at the top of the block is T_C and that at the bottom is denoted by T_H. Far away from the fracture (at both edges) the isotherms are horizontal, but close to the fracture itself they are deformed due to the thermal conductivity differences between the fluid inside the fracture and the block material. The way in which the isotherms change and their effect on the convective flow will be discussed below, first for the fluid-filled vug, then for a fluid-filled slim fracture, and finally for the saturated porous layer. Incidentally, Wang et al. (1987) have considered the case of a vertical slab embedded in a finite block under a vertical temperature gradient. The existence of a set of critical Rayleigh numbers, depending on the depth of the block, was reported there. However, the inclined fracture always induces a global convective flow, independent of the Rayleigh number.

In Fig. 1b, the experimental setup is shown schematically. The plate is a metallic block where a vug-like or fracture-like hole has been drilled. The thermal gradient was established using thermal baths and channels in the upper and lower sides. The fluids employed were water and glycerine. Particle image velocimetry was used to measure the velocity field and the temperature contours were obtained with an infrared camera.

2.1. Fluid-filled Slab

Three different coordinate systems are used as shown in Fig. 1a. The first one corresponding to the fracture (x^*, y^*) and the other two for the left- (x_1^*, y_1^*) and right-hand (x_2^*, y_2^*) sides of the solid matrix. The Boussinesq approximation has been assumed to be valid. The steady-state momentum balance equations for the fluid inside the fracture are given by

$$\rho_0\left(u^*\frac{\partial u^*}{\partial x^*}+v^*\frac{\partial u^*}{\partial y^*}\right) = -\frac{\partial p^*}{\partial x^*}+\mu\left(\frac{\partial^2 u^*}{\partial x^{*2}}+\frac{\partial^2 u^*}{\partial y^{*2}}\right)-\rho^*(T)g_x \qquad (1)$$

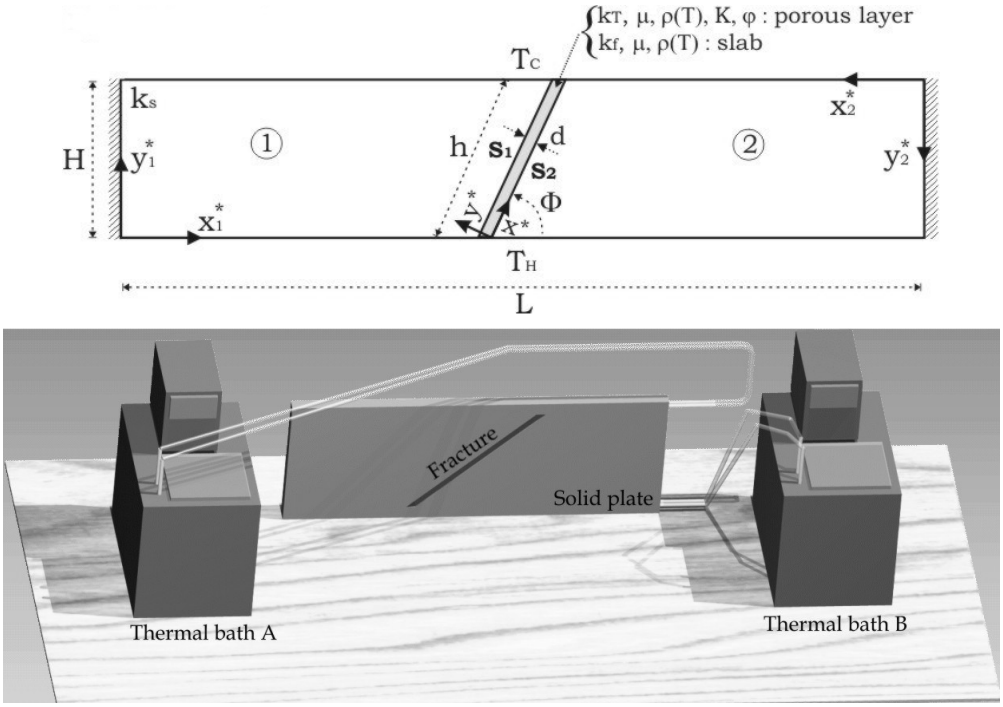

Figure 1. a) A schematic view of a rock block where a fracture (porous layer) of width d and length h is inclined respective to the horizontal plane at an angle Φ. The overall block is under a temperature difference ΔT along the vertical height H. It is important to notice that at the block edges the gradient is constant when the length L is large enough. Numbers 1 and 2 refer to the LHS and the RHS, respectively, of the block. b) The experimental setup is shown schematically.

$$\rho_0\left(u^*\frac{\partial v^*}{\partial x^*}+v^*\frac{\partial v^*}{\partial y^*}\right) = -\frac{\partial p^*}{\partial y^*}+\mu\left(\frac{\partial^2 v^*}{\partial x^{*2}}+\frac{\partial^2 v^*}{\partial y^{*2}}\right)-\rho^*(T)g_y \tag{2}$$

for the longitudinal and transverse direction, respectively. The mass conservation equation for the assumed incompressible fluid is

$$\left(\frac{\partial u^*}{\partial x^*}+\frac{\partial v^*}{\partial y^*}\right)=0 \tag{3}$$

whereas the energy conservation equation is written as

$$\rho_0 c_v\left(u^*\frac{\partial T}{\partial x^*}+v^*\frac{\partial T}{\partial y^*}\right)=k_f\left(\frac{\partial^2 T}{\partial x^{*2}}+\frac{\partial^2 T}{\partial y^{*2}}\right) \tag{4}$$

This set of governing equations must to be solved together with the following boundary conditions. Fluid adherence to the fracture walls

$$u^*=v^*=0 \quad \text{at} \quad x^*+y^*/\tan\phi=0\,,\quad x^*+y^*/\tan\phi=h \quad \text{and} \quad y^*=0,\,d \tag{5}$$

and temperature continuity at the fracture walls

$$\begin{aligned} &T=T_H && \text{at}\ \ x^*+y^*/\tan\Phi=0\,,\\ &T=T_C && \text{at}\ \ x^*+y^*/\tan\Phi=h\,,\\ &T=T_2(S_2) && \text{at}\ \ y^*=0\,,\\ &T=T_1(S_1) && \text{at}\ \ y^*=d \end{aligned} \tag{6}$$

Here S_i is the interface along $yb_i^*=(1-L/H\tan\Phi)H/2+x_i^*\tan\Phi$, where $i=1,2$.

2.2. Heat Conduction in the Rock

The solid obeys the Laplace equation in both solid blocks

$$\left(\frac{\partial^2 T_i}{\partial x_i^{*2}}+\frac{\partial^2 T_i}{\partial y_i^{*2}}\right) \quad \text{for} \quad i=1,2 \tag{7}$$

where the subscript i is referred to each part of the solid (i = 1 for the LHS and i = 2 for the RHS). Equations (7) will be solved with the boundary conditions imposed on each part of the solid. For the left- (right-) hand side block: constant temperature T_H at the top, constant temperature T_C at the bottom, adiabatic edge on the left- (right-) hand side, continuity of temperature and heat flux at S_1 (S_2):

$$\begin{aligned}
&T_i = T_H \qquad \text{at} \qquad y_i^* = (i-1)H,\\
&T_i = T_C \qquad \text{at} \qquad y_i^* = (2-i)H,\\
&\frac{\partial T_i}{\partial x_i^*} = 0 \qquad \text{at} \qquad x_i^* = 0,\\
&k_s \left.\frac{\partial T_i}{\partial n_i}\right|_{S_i} = k_f \left.\frac{\partial T_i}{\partial y^*}\right|_{y^*=(2-i)d}
\end{aligned} \tag{8}$$

Here $n_i = (h/2 - x_i)\sin\Phi - y_i\cos\Phi$ denotes the normal coordinate to the fracture walls pointing in the direction of solid i. By considering the dimensionless form of the equations, some useful approximations are introduced in the study of convection within several types of slabs embedded in the rock.

2.3. Dimensionless Equations

2.3.1 Fluid inside the fracture:

The following dimensionless variables for the spatial coordinates, velocity field, and temperatures are introduced as

$$x = \frac{x^*}{h}, \quad y = \frac{y^*}{d}, \quad u = \frac{u^* d}{\mathrm{Ra}\,\nu},$$

$$v = \frac{v^* d}{\mathrm{Ra}\,\Gamma\nu}, \quad \theta = \frac{T - T_C}{\Delta T} \tag{9}$$

respectively. The nondimensional parameters arising in this formulation are the aspect ratio Γ, the Rayleigh number Ra, and the Prandtl number Pr defined, respectively, as

$$\Gamma = \frac{d}{h}, \quad \mathrm{Ra} = \frac{g\beta\Delta T d^3 \rho_0 c_\nu}{k_f \nu}, \quad \mathrm{Pr} = \frac{\nu \rho_0 c_\nu}{k_f} \tag{10}$$

In terms of the stream function ψ ($u = \partial\psi/\partial y$, $v = -\partial\psi/\partial x$), Eqs. (1) and (2) transform into

$$\Gamma\frac{\partial\psi}{\partial y}\left[\frac{\partial^3\psi}{\partial x\partial y^2}+\Gamma^2\frac{\partial^3\psi}{\partial x^3}\right]-\Gamma\frac{\partial\psi}{\partial x}\left[\Gamma^2\frac{\partial^3\psi}{\partial x^2\partial y}+\frac{\partial^3\psi}{\partial y^3}\right]=\frac{1}{Ra}\frac{\partial^4\psi}{\partial y^4}+\frac{\Gamma^4}{Ra}\frac{\partial^4\psi}{\partial x^4}+\frac{2\Gamma^2}{Ra}\frac{\partial^4\psi}{\partial y^2\partial x^2}+\frac{\sin\Phi}{Ra\,\mathrm{Pr}}\frac{\partial\theta}{\partial y}-\frac{\Gamma\cos\Phi}{Ra\,\mathrm{Pr}}\frac{\partial\theta}{\partial x} \tag{11}$$

while the energy Eq. (3) transforms into

$$\Gamma\left[\frac{\partial\psi}{\partial y}\frac{\partial\theta}{\partial x}-\frac{\partial\psi}{\partial x}\frac{\partial\theta}{\partial y}\right]=\frac{1}{Ra\,\mathrm{Pr}}\left(\Gamma\frac{\partial^2\theta}{\partial x^2}+\frac{\partial^2\theta}{\partial y^2}\right) \tag{12}$$

The boundary conditions, Eqs. (5) and (6), take the dimensionless form

$$\begin{aligned}
&\frac{\partial\psi}{\partial x}=\frac{\partial\psi}{\partial y}=0 \qquad at \qquad \left\{\begin{matrix} x+y\Gamma\tan\Phi=0,1 \\ y=0,1 \end{matrix}\right\},\\
&\theta=1 \quad \text{at} \quad x+y\Gamma\tan\Phi=0;\\
&\theta=0 \quad \text{at} \quad x+y\Gamma\tan\Phi=1,\\
&\theta=\theta_1 \quad \text{at} \quad y=0; \qquad \theta=\theta_2 \quad \text{at} \quad y=1
\end{aligned} \tag{13}$$

2.3.2 Solid:

Introducing the nondimensional variables for the solid blocks

$$y_i = \frac{y_i^*}{H}, \quad x_i = \frac{x_i^*}{H}, \quad \theta_i = \frac{T_i - T_C}{\Delta T} \tag{14}$$

Eq. (7) yields

$$\frac{\partial^2\theta_i}{\partial x_i^2}+\frac{\partial^2\theta_i}{\partial y_i^2}=0 \quad i=1,2 \tag{15}$$

To be solved with the dimensionless form of the boundary conditions, Eq. (8), resulting

$$\begin{aligned}
&\theta_i = 1 \qquad \text{at} \qquad y_i = i-1,\\
&\theta_i = 0 \qquad \text{at} \qquad y_i = 2-i,\\
&\frac{\partial\theta_i}{\partial x_i}=0 \qquad \text{at} \qquad x_i = 0,\\
&\left.\frac{\partial\theta_i}{\partial n_i}\right|_{S_i} = \frac{\kappa\sin\Phi}{\Gamma}\left.\frac{\partial\theta}{\partial y}\right|_{y=2-i}, \qquad \theta_i(S_i)=\theta
\end{aligned} \tag{16}$$

For an oil reservoir made of limestone we have $\kappa < 1$ because in this case k_f = 0.035 cal/(m·s·K) (oil) and k_s = 0.5 cal/(m·s·K) (limestone), and so κ = 0.07 (Bear, 1972).

3. CONVECTIVE REGIMES FOR A VUG AND A FRACTURE

The ensuing analysis can be greatly simplified by considering the cases for low Rayleigh numbers and additionally: (*a*) aspect ratio Γ of the order of 10^{-1} but much larger than the ratio of conductivities κ, and (*b*) aspect ratio Γ very low compared with the ratio of conductivities κ. The cavity of case a that satisfies the specified conditions is considered here as a vug (note that the definition of a vug arises from a geometrical point of view, instead of coming from a dissolution process). Both cases studied occur very frequently in fractured reservoirs and, because of their importance, they will be treated in detail below.

3.1. Vugs

For this limit $10^{-1} \sim \Gamma >> \kappa$, Eqs. (15) as well as in the boundary conditions, Eqs. (16), the problem of the convection can be simplified because the energy equations in the blocks become independent from the fluid equations. The resulting boundary conditions at the block-fracture interfaces transform to $\partial\theta_i/\partial n_i = 0$ at S_i. The numerical scheme can be simplified using the following nonorthogonal set of transformations for $i = 1, 2$

$$\xi_i = \frac{x_i}{F_i}, \qquad F_i(y_i) = \frac{x_a}{H} - \frac{(1-y_i)}{\tan\Phi},$$
$$x_a = \frac{L + H^2 - h^2 - d/\cos\Phi}{2} \tag{17}$$

where the blocks have been transformed into unit squares. The Laplace equations (15) and the corresponding boundary conditions, Eqs. (16), now are transformed to

$$\frac{\tan^2\Phi + \xi_i^2}{F_i^2\tan^2\Phi}\frac{\partial^2\theta_i}{\partial\xi_i^2} + \frac{2\xi_i}{F_i^2\tan^2\Phi}\frac{\partial\theta_i}{\partial\xi_i} - \frac{2\xi_i}{F_i\tan\Phi}\frac{\partial^2\theta_i}{\partial y_i\partial\xi_i} + \frac{\partial^2\theta_i}{\partial y_i^2} = 0 \tag{18}$$

and

$$\theta_i(y_i = 0) = 2 - i, \qquad \theta_i(y_i = 1) = 1 - i,$$
$$\left.\frac{\partial\theta_i}{\partial\xi_i}\right|_{\xi_i=0} = 0, \qquad \left.\frac{2}{F_i\sin(2\Phi)}\frac{\partial\theta_i}{\partial\xi_i}\right|_{\xi_i=1} = \left.\frac{\partial\theta_i}{\partial y_i}\right|_{\xi_i=1} \tag{19}$$

Equations (18) with the boundary conditions, Eqs. (19), have been numerically solved using conventional centered finite differences. An alternative method called *boundary integral equation method* (BIEM) (Ligget et al., 1988) is very useful for the numerical solution of harmonic equations in complex geometries, and thus it was employed to solve the above equations obtaining similar results. In the same way, the dimensionless energy equation for the fluid, Eq. (12), under the approximations given above yields $\partial^2\theta/\partial y^2 = 0$, whose solution is given by

$$\theta = \theta(x) + [\theta_2(S_2) - \theta_1(S1)]y \tag{20}$$

Here, $\theta_i(S_i)$ are the numerical values of the nondimensional temperature at the RHS and at LHS block-fracture interfaces, respectively. In Fig. 2, a direct comparison between

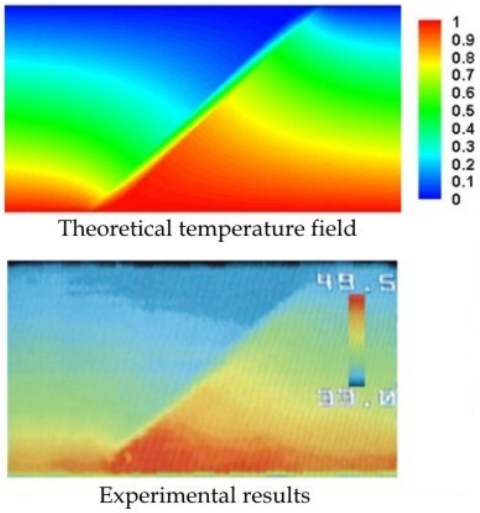

Figure 2. Experimental and theoretical temperature profiles inside the vug and in the blocks.

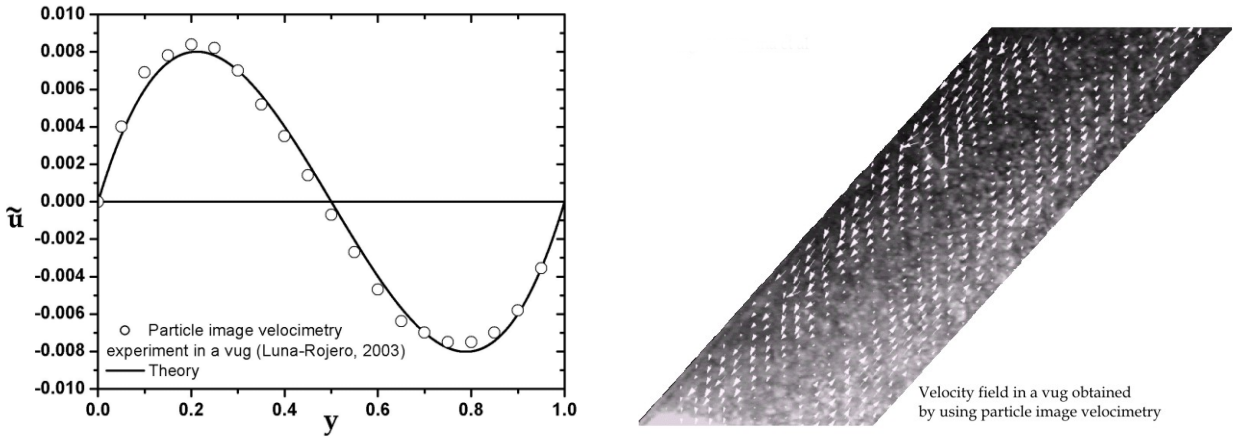

Figure 3. a) Experimental and theoretical dimensionless velocity profile $\tilde{u}$ as a function of y in a vug or in a fracture. b) Velocity field in a vug obtained with particle image velocimetry.

an actual temperature distribution (infrared image), obtained from a solid block having a fluid-filled vug, and the theoretical temperature profiles are given. As is evident in such a figure, the agreement between these dimensionless temperature fields is good. This actual temperature distribution was taken from Luna-Rojero (2003) where the assumed conditions in the theoretical model were achieved.

By the way, the nondimensional momentum equation for the fluid, Eq. (11), in the above approximation reduces to

$$\frac{\partial^2 \psi}{\partial y^4} = \frac{\sin \Phi \, [\theta_2(S_2) - \theta_1(S_1)]}{\mathrm{Pr}} \tag{21}$$

or in terms of the velocity,

$$\frac{d^2 u}{dy^3} = \frac{\sin \Phi \, [\theta_2(S_2) - \theta_1(S_1)]}{\mathrm{Pr}} \tag{22}$$

which is solved with the boundary conditions given by Eqs. (13). The solution for the velocity in the approximation of a very low Rayleigh number for the flow within the vug yields

$$u = \frac{\partial \psi}{\partial y} = \frac{\sin \Phi [\theta_2(S_2) - \theta_1(S_1)]}{12\mathrm{Pr}} (2y^3 - 3y^2 + y) \tag{23}$$

$$\tilde{u} = u / \left| [\theta_2(S_2) - \theta_1(S_1)] \sin \Phi / (12\mathrm{Pr}) \right|$$

[T1]and the experimental data for a Rayleigh number Ra = 0.9 are plotted in Fig. 3a. In Fig 3b is shown the velocity field obtained with particle image velocimetry. Notice that this profile exists for any value of Ra and, consequently, it occurs at any temperature difference. The agreement between theory and experiments, including the temperature profiles, is excellent. The symmetric flow already has been observed in experiments (Luna et al., 2002; Luna-Rojero, 2003). Having this confidence in our approach, we also treat the case of a tilted, slim fracture in the following subsection.

3.2. Fracture

The typical fractures in a reservoir have very small aspect ratios compared with unity. In this case, the ratio of thermal conductivities κ is assumed to be very large compared with Γ. In this parametric region, the fluid and block equations are coupled (contrary to the vug problem). The solution in this regime can be obtained by using a combination of asymptotic analysis together with the BIEM code. Thus, the solution for the nondimensional temperature of the blocks θ_i, the temperature in the fluid θ_f, and the stream function ψ are assumed to be given by the following asymptotic series

$$\begin{aligned} \theta_i &= \theta_{i,0} + \Gamma \theta_{i,1} + O(\Gamma^2) \, , \\ \theta &= \theta_{f0} + \Gamma \theta_{f1} + O(\Gamma^2) \, , \\ \psi &= \psi_0 + \Gamma \psi_1 + O(\Gamma^2) \end{aligned} \tag{24}$$

Introducing Eqs. (24) into Eqs. (11), (12), and (15) and the corresponding boundary conditions, Eqs. (13) and

(16), yields the following set of equations for the leading order in Γ

$$\frac{\partial^2 \theta_{f0}}{\partial y^2} = 0 \tag{25}$$

$$\frac{\partial^4 \psi_0}{\partial y^4} + \frac{\sin \Phi}{\mathrm{Pr}} \frac{\partial \theta_{f0}}{\partial y} = 0 \tag{26}$$

$$\frac{\partial^2 \theta_{i,0}}{\partial x_i^2} + \frac{\partial^2 \theta_{i,0}}{\partial y_i^2} = 0 \tag{27}$$

The first-order correction equations take the form

$$\mathrm{Ra}\left[\frac{\partial \psi_0}{\partial y}\frac{\partial \theta_{f0}}{\partial x} - \frac{\partial \psi_0}{\partial x}\frac{\partial \theta_{f0}}{\partial y}\right] = \frac{1}{\mathrm{Pr}}\left(\frac{\partial^2 \theta_{f0}}{\partial x^2} + \frac{\partial^2 \theta_{f1}}{\partial y^2}\right) \tag{28}$$

$$\mathrm{Ra}\left[\frac{\partial \psi_0}{\partial y}\frac{\partial^3 \psi_0}{\partial x \partial y^2} - \frac{\partial \psi_0}{\partial x}\frac{\partial^3 \psi_0}{\partial y^3}\right] = \frac{\partial^4 \psi_1}{\partial y^4} + \frac{\cos(\Phi)}{\mathrm{Pr}}\frac{\partial \theta_{f1}}{\partial y} - \frac{\sin(\Phi)}{\mathrm{Pr}}\frac{\partial \theta_{f0}}{\partial x} \tag{29}$$

$$\frac{\partial^2 \theta_{i,1}}{\partial x_i^2} + \frac{\partial^2 \theta_{i,1}}{\partial y_i^2} = 0 \tag{30}$$

with the boundary conditions

$$\begin{aligned}
&\theta_{i,0} = 2 - i \quad \text{and} \quad \theta_{i,1} = 0 \quad \text{at} \quad y_i = 0,\\
&\theta_{i,0} = 1 - i \quad \text{and} \quad \theta_{i,1} = 0 \quad \text{at} \quad y_i = 1,\\
&\frac{\partial \theta_{i,0}}{\partial x_i} = 0 = \frac{\partial \theta_{i,1}}{\partial x_i} \quad \text{at} \quad x_i = 0,\\
&\frac{\partial \theta_{f0}}{\partial y} = 0 \quad \text{at} \quad S_i,\\
&\theta_{i,0} = \theta_{f0} \quad \text{and} \quad \theta_{i,1} = \theta_{f1} \quad \text{at} \quad S_i
\end{aligned} \tag{31}$$

Moreover, the stick condition on the fracture walls yields

$$\frac{\partial \psi_0}{\partial x} = \frac{\partial \psi_1}{\partial x} = \frac{\partial \psi_0}{\partial y} = \frac{\partial \psi_1}{\partial y} = 0 \quad \text{at} \quad S_i \tag{32}$$

The solutions up to the first order in are given by:

$$\theta_1 = 1 - y_1 + \frac{\Gamma}{2\kappa \tan \Phi}\Theta_1(x_1, y_1) + O(\Gamma^2) \tag{33}$$

$$\theta_2 = y_2 + \frac{\Gamma}{2\kappa \tan \Phi}\Theta_2(x_2, y_2) + O(\Gamma^2) \tag{34}$$

$$u = \frac{1}{12\,\mathrm{Pr}}\left(\frac{1}{\kappa} - 1\right)\Gamma \cos\Phi\left[2y^3 - 3y^2 + y\right] + O(\Gamma^2),$$

$$v = 0 + O(\Gamma^2) \tag{35}$$

$$\theta = 1 - x + \frac{\Gamma}{\kappa \tan \Phi}\left(\frac{1}{2} - y\right) + O(\Gamma^2) \tag{36}$$

where Θ_1 and Θ_2 are functions obtained by solving the Laplace equations

$$\frac{\partial^2 \Theta}{\partial x_i^2} + \frac{\partial^2 \Theta_i}{\partial y_i^2} = 0\,, \quad \text{for} \quad i = 1, 2 \tag{37}$$

with the boundary conditions

$$\begin{aligned}
&\Theta_i = 0 \quad \text{at} \quad y_i = 0 \quad \text{and} \quad y_i = 1\\
&\frac{\partial \Theta_i}{\partial x_i} = 0 \quad \text{at} \quad x_i = 0,\\
&\Theta_i = (-1)^i \quad \text{at} \quad S_i
\end{aligned} \tag{38}$$

The BIEM method has been employed to find Θ_1 and Θ_2 in a tilted fracture, for the concrete case $\Phi = \pi/4$ and $\Gamma/\kappa = 0.01$. The dimensionless velocity $\tilde{u} = u/[(1/\kappa - 1)\Gamma \cos \Phi/(12\ \mathrm{Pr})]$ is shown graphically in Fig. 3a and it is similar to the vug case. The experimental infrared image and the theoretical dimensionless temperature contours are in excellent agreement (Fig. 4).

4. CONVECTION IN A SATURATED POROUS LAYER

The problem of the saturated, tilted porous layer is geometrically similar to that shown in Fig. 1. However, in the present case, the fracture is replaced by a thin porous layer ($\Gamma = d/h << 1$) embedded in the block, with permeability K and porosity φ. The viscosity and density of the fluid (oil) inside the porous layer are μ and ρ, respectively. The overall thermal diffusivity of the oil-saturated porous medium is designated by k_T, then for this case $\kappa = k_T/k_s$. In the limit of a thin porous layer, the transversal velocity component is small in comparison to the longitudinal velocity, which in a wide zone is only dependent on the transverse coordinate y^*. The nondimensional governing equations for the problem considered in the porous layer are given by

$$\frac{\partial u}{\partial y} = \Gamma \cos \Phi \frac{\partial \theta}{\partial x} - \frac{\partial \theta}{\partial y} \sin \Phi \tag{39}$$

$$\int_0^1 u\,dy = 0 \tag{40}$$

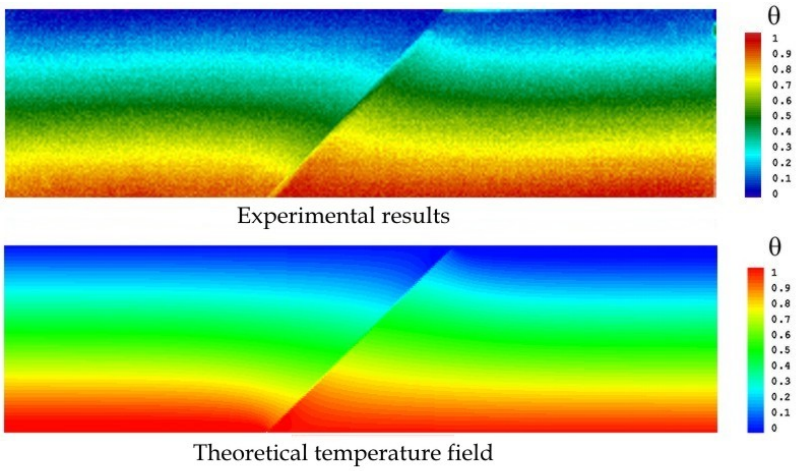

Figure 4. Experimental and theoretical dimensionless temperature profiles (θ_1 and θ_2) in the solid block and in the slim fracture or a porous layer (θ)

$$\mathrm{Ra}\,\Gamma u\frac{\partial\theta}{\partial x}=\Gamma^2\frac{\partial^2\theta}{\partial x^2}-\frac{\partial^2\theta}{\partial y^2} \tag{41}$$

where the Darcy–Boussinesq flow model has been used, considering the gravity. The pressure has been removed by combining the horizontal and vertical Darcy equations. The density in the fluid is assumed to be linearly dependent of temperature $\rho = \rho_0 - \beta\,(T - T_f)$, where ρ_0 is the density at a reference temperature and β is the thermal volume expansion coefficient. The nondimensional variables are given by

$$u=\frac{\mu u^*}{K\rho_0\beta\Delta T g} \tag{42}$$

and the Rayleigh number for the flow in the porous medium is now defined by

$$\mathrm{Ra}=\frac{K\rho_0\beta g\Delta T d}{k_T\mu} \tag{43}$$

The nondimensional boundary conditions for the temperature of the fluid in the porous medium are similar to the case studied previously and given by Eq. (13). The block equations are defined as in Eqs. (15) and (16).

4.1. Asymptotic Solution

For values of $\Gamma << 1$, the solution of this regular problem can be obtained using Γ as the small parameter of expansion, in the form

$$\begin{aligned} u &= u_0+\Gamma u_1+O(\Gamma^2),\\ \theta &= \theta_{f,0}+\Gamma\theta_{f,1}+O(\Gamma^2),\\ \theta_i &= \theta_{i,0}+\Gamma\theta_{i,1}+O(\Gamma^2) \end{aligned} \tag{44}$$

The solution up to a term of order Γ are given by

$$\begin{aligned} u &= \Gamma\cos(\Phi)\left[\frac{1}{\kappa}-1\right]\left(y-\frac{1}{2}\right)+O\left(\Gamma^2\right)\\ \theta &= 1-x+\frac{\Gamma}{\kappa\tan(\Phi)}\left(\frac{1}{2}-y\right)+O\left(\Gamma^2\right) \end{aligned} \tag{45}$$

$$\begin{aligned} \theta_1 &= 1-y_1+\frac{\Gamma}{2\kappa\tan(\Phi)}\Theta_1(y_1,x_1)+O(\Gamma^2)\\ \theta_2 &= y_2+\frac{\Gamma}{2\kappa\tan(\Phi)}\Theta_2(y_2,x_2)+O(\Gamma^2) \end{aligned} \tag{46}$$

Here Θ_1 and Θ_2 have to be determined by the solution of the Laplace equation (37) with the boundary conditions defined in Eq. (38). Again the BIEM method has been employed to find Θ_1 and Θ_2. The dimensionless temperature profiles in this case are similar to those obtained for the case of the slim fracture (see, Fig. 4 for the temperature within the porous layer and the temperatures in the solid blocks).

5. PASSIVE DISPERSION AND DIFFUSION IN THE CAVITIES

Passive dispersion is a very important phenomenon related to the transport of contaminants and occurs when the

physical properties of the fluid do not change due to the concentration variations (Woods et al., 1992; Linz et al., 1992). Here, the dispersion due to the combined action of molecular diffusion and convection in both a tilted fracture and a porous layer have been analyzed in order to know how any contaminant is transported in these finite systems. The study of these transport phenomena is very important in the oil industry as, for example, in the passive transportation of nitrogen in some enhanced oil recovery processes. Quantitative estimates are given below for the case of nitrogen in contact with oil at the top of the fracture under reservoir conditions with realistic fractures and porous layers in Mexican, naturally fractured oil fields.

5.1. Taylor Dispersion in Fluid-filled Fractures

Following the Taylor analysis (Taylor, 1953) on the effect of the molecular diffusion on the dispersion, it is possible in the present work to write the equation of diffusion in the form

$$\frac{\partial C^*}{\partial t^*} + u^* \frac{\partial C^*}{\partial x^*} = D\left[\frac{\partial^2 C^*}{\partial x^{*2}} + \frac{\partial^2 C^*}{\partial y^{*2}}\right]$$

$$\text{and} \quad C^* + C_{\text{fluid}} = 1 \tag{47}$$

where C^* and C^*_{fluid} are, respectively, the mass concentration of the contaminant (N_2) and the fluid, u^* is the longitudinal convective velocity, t^* is the time, and D is the binary (N_2/oil) coefficient of molecular diffusion which is assumed to be independent of C^*. As in the Taylor work, here it is valid to assume that the transverse velocity component is negligibly small and it can be dropped. The boundary conditions for solving Eq. (47) are the following: the concentration at the top of the fracture is given by $C^* = C_{N2}$. The conditions at the nonpermeable interface fracture-solid block are $\partial C^*/\partial x^* = 0$ at $x^* + y^* \tan\Phi = 0$ and $\partial C^*/\partial y^* = 0$ at $y^* = 0, d$. The assumed initial condition is that the contaminant is absent at $t^* = 0$. The nondimensional form of Eq. (47) can be written as

$$\Gamma^2 \frac{\partial Y}{\partial \sigma} + \frac{\text{Pe}\Gamma^2 \cos\Phi}{\text{Pr}}\left(\frac{1}{\kappa} - 1\right) \times \left[\frac{1}{12}y + \frac{1}{6}y^3 - \frac{1}{4}y^2\right]\frac{\partial Y}{\partial x} = \left[\Gamma^2 \frac{\partial^2 Y}{\partial x^2} + \frac{\partial^2 Y}{\partial y^2}\right] \tag{48}$$

where $y = y^*/d, x = x^*/h, u = u^* d/(\text{Ra}\, v), \sigma = t^* D/h^2$, and $Y = C^*/C^*_{N2}$. $\text{Pe} = u_c d/D$ is the diffusive Peclet number and relates the characteristic transverse diffusion time to the convective time. The nondimensional boundary conditions are now written as

$$\left.\frac{\partial Y}{\partial y}\right|_{y=0,1} = \left.\frac{\partial Y}{\partial x}\right|_{x+y\Gamma\tan\Phi=0} = Y(x, y, 0) = Y(1 - y\Gamma\tan\Phi, y, \sigma)\Big| - 1 = 0 \tag{49}$$

Nitrogen is convected and diffused down by the flow coming down in the upper part of the fracture. At the same time, it also diffuses in the transverse direction, reaching positions where the convective flow moves up, thus reducing the global effect of transporting nitrogen down along the fracture. In typical oil reservoirs, the diffusive Peclet number is of the order unity or lower. In order to solve Eqs. (48) and (49), a solution of the form

$$Y = Y_0 + \Gamma^2 Y_1 + O(\Gamma^4) \tag{50}$$

is assumed, for small values of compared with unity. Introducing Eq. (50) into Eq. (48), the following set of equations are obtained

$$\frac{\partial^2 Y_0}{\partial y^2} = 0 \tag{50a}$$

$$\frac{\partial^2 \text{Y}_{\text{j+1}}}{\partial \text{y}^2} = \frac{\partial \text{Y}_\text{j}}{\partial \sigma} - \frac{\partial^2 \text{Y}_\text{j}}{\partial \text{x}^2} + \frac{\text{Pe}\cos\Phi}{12\,\text{Pr}}\left(\tfrac{1}{\kappa} - 1\right)\left(\text{y} + 2\text{y}^3 - 3\text{y}^2\right)\frac{\partial \text{Y}_\text{j}}{\partial \text{x}},$$

$$j = 0, 1, 2, \ldots \tag{51b}$$

Equation (51a) gives $Y_0(x, \sigma)$. Integrating Eq. (51b) for $j = 0$ in the transverse direction, gives

$$\frac{\partial Y_0}{\partial \sigma} = \frac{\partial^2 Y_0}{\partial x^2} \tag{52}$$

where Y_0 satisfies the classical diffusion equation, where convection plays no role at all. The solution of Eq. (52) is given by

$$Y_0 = 1 - \frac{4}{\pi}\sum_{m=1}^{\infty} \frac{\sin\left(\left(m - \tfrac{1}{2}\right)(1 - x)\pi\right)}{2m - 1} e^{-(m-1/2)^2 \pi^2 \sigma} \tag{53}$$

The $j = 1$ equation in Eq. (51b) now takes the form

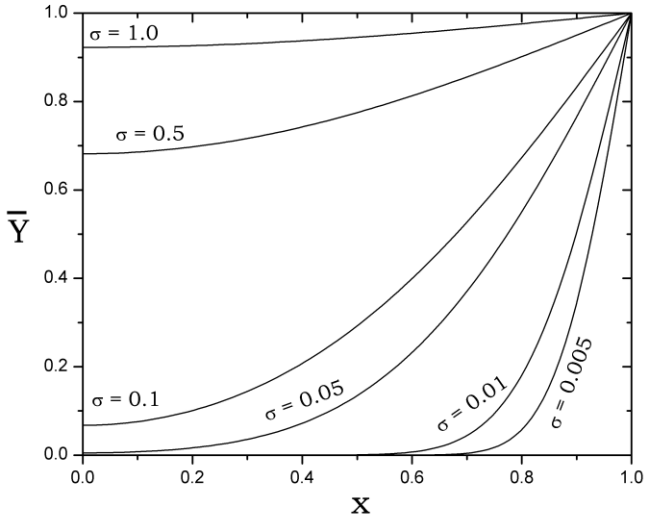

Figure 5. Results for the spatially averaged concentration $\bar{Y}(x, \sigma = \int_0^1 Y dy$ in a slim fracture saturated with oil and when N_2 was introduced at its upper part, at different nondimensional times

$$\frac{\partial^2 Y_1}{\partial y^2} = \frac{\mathrm{Pe}\left(\frac{1}{\kappa}-1\right)\cos\Phi}{12\,\mathrm{Pr}}\left(y+2y^3-3y^2\right)\frac{\partial Y_0}{\partial x} \tag{54}$$

Equation (54) can be integrated, resulting in

$$Y_1 = \frac{-\mathrm{Pe}\left(\frac{1}{\kappa}-1\right)\cos\Phi}{12\,\mathrm{Pr}}\left(\frac{y^3}{3}+\frac{y^5}{5}-\frac{y^4}{2}\right) \times\sum_{m=1}^{\infty}\cos\left(\left(m-\tfrac{1}{2}\right)(1-x)\pi\right)e^{-\left(m-\frac{1}{2}\right)^2\pi^2\sigma}+G_1 \tag{55}$$

where $G_1(x, \sigma)$ has to be obtained for $j = 2$:

$$G_1 = \frac{\mathrm{Pe}^2\left(\frac{1}{\kappa}-1\right)^2\cos^2\Phi}{362880\,\mathrm{Pr}^2}\sigma\pi \times\sum_{m=1}^{\infty}(2m-1)\sin\left(\left(m-\tfrac{1}{2}\right)(1-x)\pi\right)e^{-\left(m-\frac{1}{2}\right)^2\pi^2\sigma} \tag{56}$$

Equations (55) and (56) show the influence of convection in the diffusive transport of a passive scalar in this type of flow, which is extremely small and of the order of Γ for $\Gamma << 1$.

In Fig. 5, the results for $\bar{Y}(x, \sigma) = \int_0^1 Y dy$ corresponding to a fracture filled with oil are shown. Here the assumed diffusion coefficient has been set to $D = 3.5 \times 10^{-5}$ cm2/s (Luna et al., 2003) and the conductivities ratio to $\kappa = 0.07$. In the plot, a characteristic value of the aspect ratio, $\Gamma = 0.1$ has been employed at different nondimensional elapsed times. In two years, the oil inside the fracture travels, due to natural convection, about 170 m, but nitrogen only travels a couple of meters, mainly due to molecular diffusion. Convection shows an extremely weak influence in the way passive contaminants (nitrogen) can be dispersed in fractured media.

5.2. Dispersion in a Porous Layer

As in the previous case of a tilted fracture, the dispersion of passive material in a saturated porous layer also can be studied if the velocity field is known. However, in this case, the form of the diffusion equation changes by including the enhanced mixing process due to the velocity fluctuations in the porous media. The species conservation equations are given by (Bear, 1972)

$$\varphi\frac{\partial C^*}{\partial t^*}+u^*\frac{\partial C^*}{\partial x^*} = \varphi D_d\left[\frac{\partial^2 C^*}{\partial x^{*2}}+\frac{\partial^2 C^*}{\partial y^{*2}}\right]+\alpha\frac{\partial C^*}{\partial y^*}\frac{\partial\left|u^*\right|}{\partial y^*}.$$

$$\text{and} \quad C^* + C^*_{\mathrm{Fluid}} = 1 \tag{57}$$

where φ is the fracture porosity, $D_d = D/\tau + \alpha\left|u^*\right|/\varphi$ is the dispersion coefficient, D is the coefficient of molecu-

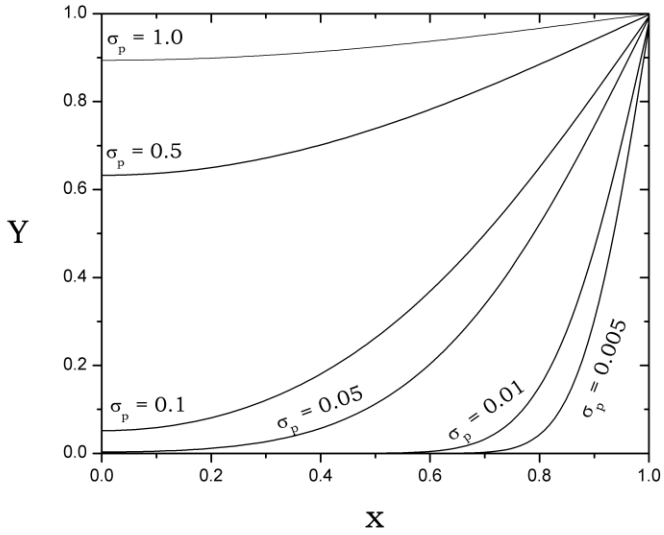

Figure 6. Dimensionless results for the dispersion in a porous layer saturated with oil and when N_2 was introduced at its upper part, at different nondimensional times

lar diffusion of the contaminant (nitrogen) in the fluid (oil) in the absence of the porous medium, τ is the tortuosity of the porous medium, and α is the longitudinal dispersivity coefficient.

Equation (57) will be solved under similar boundary and initial conditions imposed in the fluid-filled fracture given above. Using the nondimensional spatial coordinates and the concentration as above, the longitudinal velocity in the form $u = u^*/u_c = u^*/(k\rho_0\beta\Delta T_0 g/\mu)$, where u is given in Eq. (45) and the dimensionless time $\sigma_p = t^* D/h^2\tau$, the nondimensional form of Eq. (56) is given by

$$\Gamma^2\frac{\partial Y}{\partial \sigma_p}+\Gamma^2\frac{\mathrm{Pe}\left(\frac{1}{\kappa}-1\right)\cos\Phi}{\varphi}\left(y-\tfrac{1}{2}\right)\frac{\partial Y}{\partial x}=$$
$$\left(1+\Gamma\frac{\mathrm{Pe}_\alpha\left(\frac{1}{\kappa}-1\right)\cos\Phi}{\varphi}\left|y-\tfrac{1}{2}\right|\right)\left(\Gamma^2\frac{\partial^2 Y}{\partial x^2}+\frac{\partial^2 Y}{\partial y^2}\right)+$$
$$\Gamma\frac{\mathrm{Pe}_\alpha\left(\frac{1}{\kappa}-1\right)\cos\Phi}{\varphi}\frac{\partial Y}{\partial y}\frac{\partial\left|y-\frac{1}{2}\right|}{\partial y} \qquad (58)$$

where the diffusive Peclet number is $\mathrm{Pe} = d\tau u_c/D$ and the dispersive Peclet number is $\mathrm{Pe}_\alpha = \alpha\tau u_c/D$. As in the free fracture case treated before, here $\mathrm{Pe} \sim 1$ and $\mathrm{Pe}_\alpha \sim 1$. The solution is sought in the form

$$Y = Y_0 + \Gamma Y_1 + \Gamma^2 Y_2 + O(\Gamma^3) \qquad (59)$$

for small values of Γ compared with unity. The solution to Eq. (58), found by introducing the series given in (59), is given by

$$Y_0 = 1-\frac{4}{\pi}\sum_{m=1}^{\infty}\frac{\sin\left(\left(m-\frac{1}{2}\right)(1-x)\pi\right)}{2m-1}e^{-(m-1/2)^2\pi^2\sigma} \qquad (60)$$

$$Y_1 = \frac{\mathrm{Pe}_\alpha\left(\frac{1}{\kappa}-1\right)\cos\Phi}{4\varphi}\sigma_p\pi$$
$$\times\sum_{m=1}^{\infty}(2m-1)\sin\left(\left(m-\tfrac{1}{2}\right)(1-x)\pi\right)e^{-(m-1/2)^2\pi^2\sigma} \qquad (61)$$

In Fig. 6 are shown the dimensionless results for the dispersion in a porous layer saturated with oil and when N_2 was introduced at its upper part. The dispersive Peclet number was taken as $\mathrm{Pe}_\alpha = 1$. Additionally, from field data it is known that $\varphi \approx 0.15$, $\kappa \approx 0.86$, and $\tau \approx 1.2$. In Fig. 6, the assumed aspect ratio was $\Gamma = 0.1$ at different nondimensional times. In a two year period, the oil has travelled 20 m due to convection while the N_2 has only travelled a couple of meters.

6. CONCLUSIONS AND REMARKS

In this work, the problems of thermal convection in finite, oil-filled, tilted fractures and tilted porous layers, have been analyzed. In nature, fractures and layers are embedded within near-impervious porous rocks which are subjected to a geothermal gradient. Here, the influence of these structures on the temperature distribution by convection and dispersion has been studied. The theoretical treatment used in this work allows us to determine analytically

the velocity field and the temperature profiles inside these fractures and to determine the spatial evolution of the concentration of a passive scalar, considering molecular diffusion and dispersion under geothermal-driven convective flows. Cases for inclinations of fractures with an inclination angle of $\Phi = \pi/4$ and several combinations of aspect and conductivities ratio were treated and actual estimations for the dispersion in limestone oil-reservoirs were given. In this paper we have shown that the geothermal-driven convective flows inside closed fractures do not change the characteristic overall diffusion or dispersion processes of conserved scalars injected at one of the ends of the fractures. Finally, in some reservoirs it is feasible to have negative temperature gradients, i.e., the temperature decreases when the depth increases. This situation can occur naturally or artificially due to the existence of heat sources adequately localized. In such a case, the treatment here discussed is made valid by changing $\Delta T \to -\Delta T$ when it occurs. A direct and important result under this change is that the velocity profiles in all the cases here considered are inverted in sign. Moreover, this inversion in the flow direction does not change the main results related to dispersion.

ACKNOWLEDGMENTS

This work has been benefited with the financial support from the Mexican Petroleum Institute (IMP) through the projects FIES 98-58-I and D.02100 and from CONACyT through the grant NC-24.

REFERENCES

Bear, J., *Dynamics of Fluids in Porous Media*, Elsevier, New York, 1972.

Bejan, A., *Convection Heat Transfer*, Second Edition, Wiley, New York, 1995.

Davies, S. H., Rosenblat, S., Wood, J. R. and Davies, T. A., Convective fluid flow and diagenetic patterns in doomed sheets, *Am. J. Sci*., vol. 285, pp. 207–223, 1981.

Horton, C. W., and Rogers, F. T., Convection currents in a porous medium, *J. Appl. Phys*., vol. 16, pp. 367–370, 1945.

Lake, L. W., *Enhanced Oil Recovery*, Prentice Hall, Englewood Cliffs, NJ, 1989.

Lapwood, E. R., Convection of a fluid in a porous medium, *Proc. Cambridge Philos. Soc*., vol. 44, pp. 508–521, 1948.

Ligget, J. A., and Liu, P. L.-F., *The Boundary Integral Equation Method for Porous Media Flow*, Allen & Unwin, 1988.

Linz, S. J., and Woods, A. W., Natural convection, Taylor dispersion, and diagenesis in a tilted porous layer, *Phys. Rev. A*, vol. 46, pp. 4869–4878, 1992.

Luna, E., Córdova, A., Medina, A., and Higuera, F. J., Convection in a finite fracture in a rock, *Phys. Lett. A*, vol. 300, pp. 449–455, 2002.

Luna-Rojero, E., Ph.D. dissertation, Facultad de Ingenieria, UNAM, 2003.

Medina, A., Luna, E., Pérez-Rosales, C., and Higuera, F. J., Thermal convection in tilted porous fractures, *J. Phys.: Condens. Matter*, vol. 14, pp. 2467–2474, 2002.

Nield, D.A., and Bejan, A., *Convection in Porous Media*, Springer-Verlag, New York, 1998.

Phillips, O. M., *Flow and Reactions in Permeable Rocks*, Cambridge University Press, Cambridge, England, 1991.

Saffman, P. G., A theory of dispersion in a porous medium. *J. Fluid Mech*., vol. 6, pp. 321–349, 1959.

Taylor, G., Dispersion of soluble matter in a solvent flowing slowly through a tube, *Proc. R. Soc. A*, vol. 219, pp. 186–203, 1953.

Wang, M., Kassoy, D. R., and Weidman, P. D., Onset of convection in a vertical slab of saturated porous media between two impermeable conducting blocks, *Int. J. Heat Mass Transfer*, vol. 30, pp. 1331–1341, 1987.

Woods, A. W. and Linz, S. J., Natural convection and dispersion in a tilted fracture, *J. Fluid Mech*., vol. 241, pp. 59–74, 1992.